

ARMY RESEARCH LABORATORY



A Study of a Steel Right Circular
Cylinder (RCC) Striking 23 Plies
of KM2 Fabric Using the
LS-DYNA Lagrangian Hydrocode

by Dennis S. Pritchard

ARL-TR-2673

February 2002

Approved for public release; distribution is unlimited.

20020325 157

The findings in this report are not to be construed as an official Department of the Army position unless so designated by other authorized documents.

Citation of manufacturer's or trade names does not constitute an official endorsement or approval of the use thereof.

Destroy this report when it is no longer needed. Do not return it to the originator.

Army Research Laboratory

Aberdeen Proving Ground, MD 21005-5066

ARL-TR-2673

February 2002

A Study of a Steel Right Circular Cylinder (RCC) Striking 23 Plies of KM2 Fabric Using the LS-DYNA Lagrangian Hydrocode

Dennis S. Pritchard

Weapons and Materials Research Directorate, ARL

Approved for public release; distribution is unlimited.

Abstract

A study was conducted to examine the terminal effects of a 1.0-g steel RCC impacting 23 plies of KM2 fabric using the LS-DYNA Lagrangian hydrocode. The simulated impact velocities were 200, 400, 600, 800, 1000, 1200, and 1400 m/s. The fabric was a plain weave of 850 denier yarn. The LS-DYNA-simulated V_s versus V_r data points generated at the U.S. Army Research Laboratory (ARL) were compared to both experimental data and EPIC-generated data. Also, the LS-POST software package was used to view the simulated physical descriptions of the penetrator and target at various stages of the penetration process.

Acknowledgments

This work was supported in part by a grant of computer time from the DOD High Performance Computing Modernization Program at Aberdeen Proving Ground, MD. Mr. D. Grove is gratefully acknowledged for his efforts in support of the work reported here.

INTENTIONALLY LEFT BLANK.

Contents

Acknowledgments	iii
List of Figures	vii
List of Tables	ix
1. Introduction	1
2. Review and Analysis	1
2.1 Experimental Data	1
2.2 LS-DYNA Simulations	4
2.3 EPIC Simulations	6
3. Summary	15
4. References	17
Appendix A. LS-Ingrid Input Deck for RCC and 23-Ply Target	19
Appendix B. Abbreviated LS-DYNA Input Deck for RCC Impacting 23-Ply Target ($V_s = 200$ m/s)	25
Distribution List	41
Report Documentation Page	43

INTENTIONALLY LEFT BLANK.

List of Figures

Figure 1. Comparison of simulation results with experimental V_s versus V_r data.....	2
Figure 2. LS-DYNA RCC and target simulation grid prior to impact ($V_s = 200$ m/s).....	7
Figure 3. LS-DYNA simulation at 70 μ s into run showing damage up to the fifth ply ($V_s = 200$ m/s).	8
Figure 4. LS-DYNA simulation at 70 μ s into run showing damage up to the sixteenth ply ($V_s = 400$ m/s).	9
Figure 5. LS-DYNA simulation at 30 μ s into run ($V_s = 600$ m/s).	10
Figure 6. LS-DYNA simulation at 30 μ s into run ($V_s = 800$ m/s).	11
Figure 7. LS-DYNA simulation at 25 μ s into run ($V_s = 1000$ m/s).	12
Figure 8. LS-DYNA simulation at 20 μ s into run ($V_s = 1200$ m/s).	13
Figure 9. LS-DYNA simulation at 15 μ s into run ($V_s = 1400$ m/s).	14

INTENTIONALLY LEFT BLANK.

List of Tables

Table 1. V_s versus V_r values.	3
Table 2. Selected material properties used in LS-DYNA input deck.	4

INTENTIONALLY LEFT BLANK.

1. Introduction

A study was conducted to examine the terminal effects of a 1.0-g steel right circular cylinder (RCC) impacting 23 plies of KM2 fabric. Simulations and analyses were conducted using the LS-DYNA Lagrangian hydrocode* in support of the Science and Technical Objective (STO) titled "Ballistic Protection for Improved Individual Survivability." This joint STO between the U.S. Army Research Laboratory (ARL) and the Natick Soldier Center is advancing materials technology to improve the protection of personnel armor systems against current and emerging fragment and bullet threats. The STO is also providing tools to benefit the development, design, and acquisition of personnel armor.

2. Review and Analysis

Experimental V_s (striking velocity) versus V_r (residual velocity) data and hydrocode simulations using LS-DYNA and EPIC are discussed in the following sections.

2.1 Experimental Data

Experimental data forms the baseline for comparison to the computed results. The experimental data from Johnson et al. (1999) are shown in Figure 1 and Table 1. The RCC, having a length-to-diameter ratio of one, struck the targeted fabric layup at 0° obliquity. It is seen that a V_{50} of approximately 600 m/s can be assigned to the experimental data. The V_{50} is defined within a narrow V_s range as the V_s that is bracketed by half of the projectiles in a test sampling in that narrow range not making it through the target layup ($V_r = 0$), balanced by a corresponding half number of projectiles barely penetrating the target layup ($V_r > 0$) in the same range. Once the exact "over" and "under" data points are determined, the V_{50} equals the average of the V_s values for these points. From an experimental standpoint of obtaining V_{50} for a particular penetrator and target configuration, this data set is exemplary, as the cost of determining the V_{50} is roughly proportional to the number of shots fired; the fewer the shots, the lower the cost. The V_{50} number often forms the decision point describing the acceptability of an armor configuration on a pass/fail basis when attacked by a particular penetrator. For a more rigorous explanation of how to experimentally find a V_{50} , the military standard MIL-STD-662E (Department of the Army 1992) should be studied. As the V_s increased, the fabric layup became less effective in stopping the RCC as a function of the fabric's decreasing ability to withstand dynamic loading.

* LS-DYNA Version 950d, Livermore, CA: Livermore Software Technology Corporation.

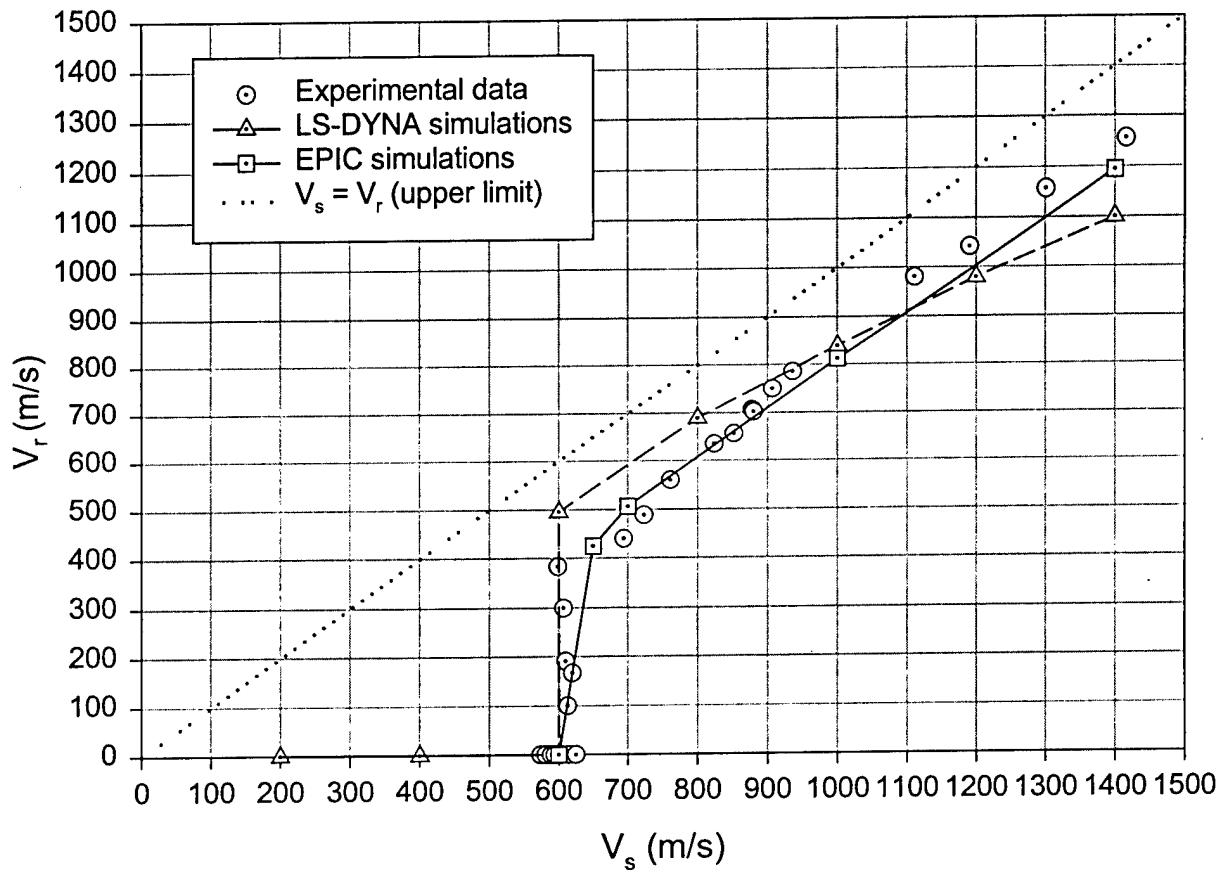


Figure 1. Comparison of simulation results with experimental V_s versus V_r data.

Table 1. V_s versus V_r values.

Experimental V_s (m/s)	Experimental V_r (m/s)	LS-DYNA V_s (m/s)	LS-DYNA V_r (m/s)	EPIC V_s (m/s)	EPIC V_r (m/s)
574	0	200	0	600	0
581	0	400	0	650	425
589	0	600	495	700	506
594	0	800	689	1000	812
599	383	1000	839	1400	1194
604	0	1200	980		
607	299	1400	1100		
610	191				
615	0				
613	100				
620	167				
625	0				
694	440				
723	488				
761	560				
824	635				
852	656				
878	706				
880	702				
907	750				
936	786				
1111	981				
1191	1042				
1301	1157				
1416	1255				

This statement is evidenced by the increase in V_r as V_s increased after the V_s value of 600 m/s had been significantly surpassed. The V_s versus V_r values starting at and including the point with the 599 m/s V_s value could reasonably be fit with a straight line that roughly parallels the $V_s = V_r$ line.

2.2 LS-DYNA Simulations

The ARL-simulated V_s versus V_r data were obtained by using LS-DYNA Version 950d and are shown in Figure 1 and Table 1. The RCC and fabric target grid generation was accomplished by running the LS-INGRID computer software package* with the ARL-designed input deck presented in Appendix A. This run gave the properly formatted (Fortran 77) node and element data that was stripped from the LS-INGRID output deck called ingrido. This stripped deck was inserted into the LS-DYNA keyword formatted deck for each LS-DYNA run, with the material property cards, among others, preformatted. A resultant typical LS-DYNA input deck used in this report, with only the extensive node and element (8-node brick) data abbreviated, is shown in Appendix B. The projectile had a total of 1331 nodes and 1000 solid elements. Each ply had 3362 nodes and 1600 solid elements, with individual element dimensions of $0.1578 \times 0.5000 \times 0.5000$ mm. The projectile and target element sizing were comparable. Each ply was one element thick, with the ply dimensions equal to $0.1578 \times 20 \times 20$ mm. Changes were made to the LS-DYNA input deck for each initial impact velocity, where at least each different impact velocity had to be specified, and some changes were required for the other material properties as shown in Table 2.

Table 2. Selected material properties used in LS-DYNA input deck.

Property	KM2 Ply ($V_s = 200$ and 400 m/s)	KM2 Ply ($V_s = 600$ m/s and up)	Steel
Density (g/cm ³)	1.438 ^a	1.438 ^a	7.87 ^b
Young's Modulus (Mbar)	0.08325	0.74	2.068395 ^c
Poisson's Ratio	0.2 ^a	0.2 ^a	0.29 ^d
Yield Stress (Mbar)	—	—	0.010342 ^c
Failure Strain	0.2	0.025	—

^a Johnson et al. (1999).

^b Lyman (1961).

^c Flinn and Trojan (1975).

^d Kolsky (1963).

The steel was modeled as an elastic-perfectly plastic material. Although many of the material properties in Table 2 were directly obtained from the listed references, explanations for the choice of others are required as follows.

The KM2 volumetric density in Table 2 was derived from constants found in the Johnson et al. (1999) paper and is close to the commonly quoted value of 1.44 g/cm³, but is not that exact value. The fabric description was modified from

* LS-INGRID Version 3.5, Livermore, CA: Livermore Software Technology Corporation.

the actual weave pattern for each ply into a plate of solid elements with nominally the same material properties as the actual ply. The volumetric density for a simulated KM2 ply is dependent on the way the change from the actual weave pattern to a solid element description is interpreted. The areal density of the experimental layup was quoted as 5.22 kg/m^2 with a modeled effective thickness (not the true experimental thickness) of 3.63 mm given by Johnson et al. (1999) for the 23 plies. These constants force each ply thickness to be 0.1578 mm and the volumetric density for this thickness to be 1.438 g/cm^3 . Since each actual ply was a plain weave of 850 denier yarn, this fact fixes the maximum total target thickness allowed. With 23 plies and 22 gaps between plies built in, this makes each gap 0.1391 mm wide to give a reasonable approximation of the total target thickness as 6.6896 mm , which was equal to the measured thickness of a 23-ply layup measured in the laboratory, within a small error band. It was thought that the solid elements with gaps between plies were required to minimize the effect of geometric nonproportionality on the simulated penetration process. One would encounter this effect by equating the 23 plies to some type of single-layer shell element description, for example.

Two quantities in Table 2 that definitely require an explanation for their origins are the Young's modulus and failure strain values. Shim et al. (2001) found, while conducting high strain-rate testing with the Split-Hopkinson Pressure Bar (SHPB), that the failure of Twaron fabric (similar to KM2 fabric) is highly strain-rate dependent with the tensile strength and modulus increasing with increasing strain rate, while the failure strain decreases with increasing strain rate. They also found that Twaron fabric failed in a more brittle manner as a function of increasing strain rate, which significantly reduced the amount of energy that could be absorbed by a particular yarn prior to its failure. This is consistent with the observed behavior described in the previous sentence. These experimental observations can be used to help describe the failure behavior of fabrics during ballistic penetration as follows. In a set of ballistic experiments, the strain rate experienced by the target material increases in some proportion to increasing projectile impact velocity, holding all other initial conditions constant. Thus, at higher impact velocities, the KM2 fabric should exhibit a higher Young's modulus and a lower strain to failure (see Table 2). Now, the Young's modulus and failure strains in Table 2 do not exactly fit the values given by Shim et al. (2001), but are extrapolated from their data. It was assumed, given the high strain rates achieved in the ballistic testing modeled in this report, that the yarns in the fabric weave could be thought to have elastic material properties to the point of failure with virtually no onset of plastic deformation. This assumption can be thought of as an elastic-perfectly brittle model. The highest modulus found for the Twaron fabric (more similar to Kevlar 29 fabric than to KM2 fabric) by Shim et al. (2001) was close to 0.74 Mbar at the highest testing strain-rate they used (495 s^{-1}). This was assumed to be a fair estimate corresponding to the strain-rate encountered on the high end of the striking velocity range of the

simulated ballistic tests with the KM2 fabric. However, KM2 fibers are somewhat tougher than Twaron or Kevlar 29 fibers, so the Shim et al. (2001) strain to failure of about 0.016 was increased to match the toughness-related increase in the ductile-to-brittle strain-to-failure criterion for the KM2 (failure strain = 0.025). Shim et al. (2001) found very low Young's moduli at the lowest end (quasi-static) of their strain-rate range (see their Figure 4). To reflect the strain-rate condition of a lower Young's modulus for a lower strain rate, a midrange-value Young's modulus was picked for the 200 and 400 m/s striking velocities as shown in Table 2. Based on the Shim et al. (2001) data values for strain-rate conditions approaching and equal to the quasi-static values for Twaron, a KM2 failure strain of 0.2 appeared to be reasonable. However, if actual SHPB data were ever obtained for KM2 fabric, the method for determining the Young's modulus and failure strain values in Table 2 would have to be readdressed.

The LS-DYNA-programmed V_s values were 200, 400, 600, 800, 1000, 1200, and 1400 m/s. The simulated penetration behavior for each V_s is visually summarized in Figures 2-9 as a product of the LS-POST software package.* For scaling purposes in these figures, it must be remembered that the projectile diameter was 5.45 mm, but this value is directly scalable only in the y-direction, as the simulations have been rotated about the y-axis to enhance the view of the deformation of the projectile and the failure of the target material. With the 200 m/s V_s , five simulated plies were penetrated and only severe deformation without failure occurred in all remaining plies. Obviously, the condition that no part of the projectile exits the last ply was met exactly for a "no perforation" condition. For the 400 m/s V_s , significantly more simulated plies (16) were penetrated than at the 200 m/s V_s , which is consistent with the fact that deeper penetration occurs experimentally as the striking velocity increases; the "no perforation" condition was still met. For V_s of 600 m/s and above, the V_r was determined by tracking, in time, the velocity of the center rear node on the back of the RCC. When the projectile's rear surface velocity converged sufficiently to a constant velocity after penetration, that velocity was picked for the V_r .

2.3 EPIC Simulations

The EPIC-simulated V_s versus V_r points from Johnson et al. (1999) are shown in Figure 1 and Table 1. Comparisons to the LS-DYNA results can be made. For example, the difference between the V_r values for the 600 m/s V_s runs is not a major disparity, since any V_r in that vicinity has been shown experimentally to be a difficult number to interpret also. Hydrocodes do not predict V_r values at or near the experimentally determined V_{50} , a meta-stable point in the true penetration process, with accuracy any better than that found experimentally. Experimental anomalies occur near the V_{50} because of subtle shot-to-shot

* LS-POST Version 1.0, Livermore, CA: Livermore Software Technology Corporation.

RCC(1.04GM); 0.02 CM/MICROSEC;23PLY KM2
Time = 0

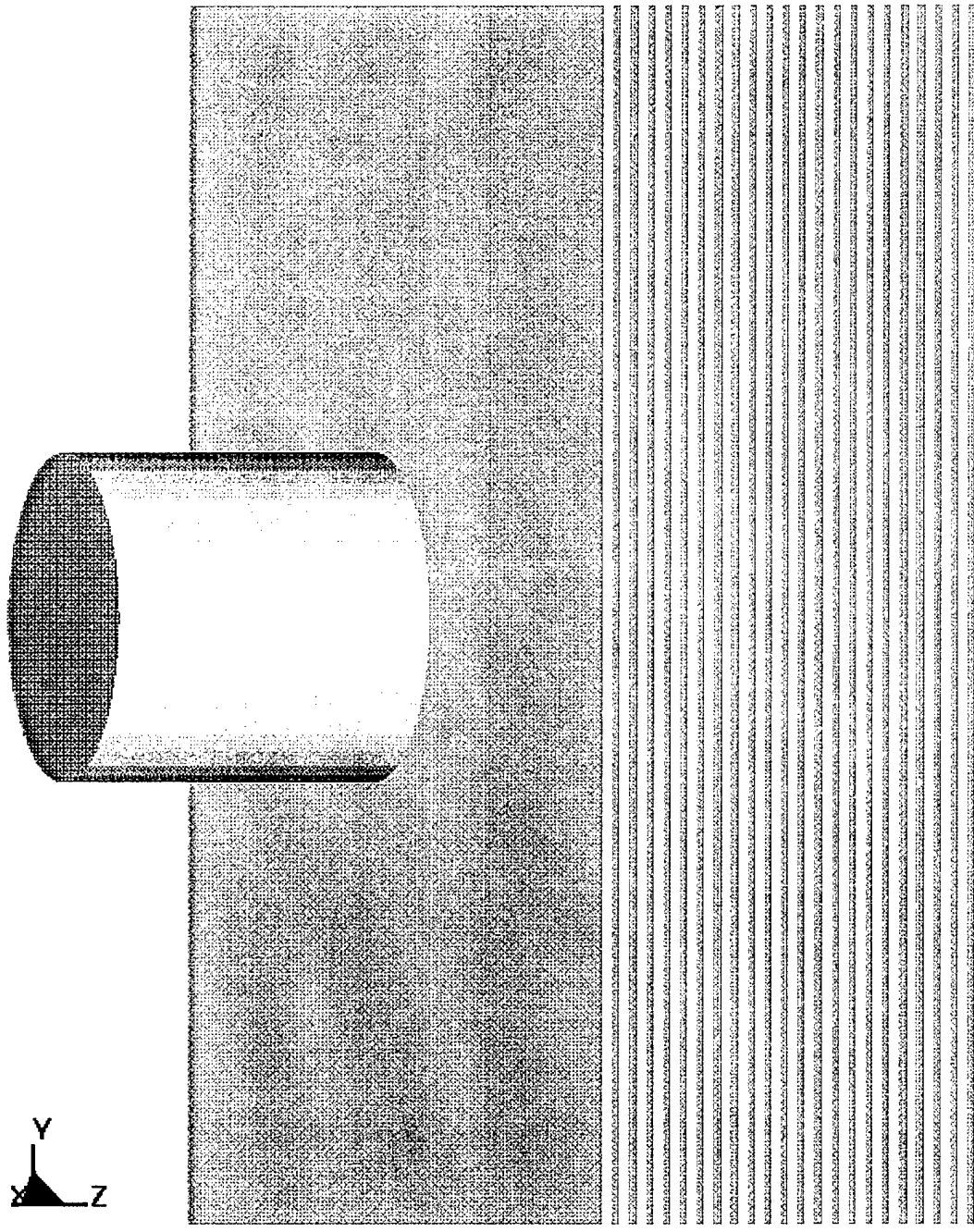


Figure 2. LS-DYNA RCC and target simulation grid prior to impact ($V_s = 200$ m/s).

RCC(1.04GM); 0.02 CM/MICROSEC;23PLY KM2
Time = 70



Figure 3. LS-DYNA simulation at 70 μ s into run showing damage up to the fifth ply ($V_s = 200$ m/s).

RCC(1.04GM); 0.04 CM/MICROSEC;23PLY KM2
Time = 70

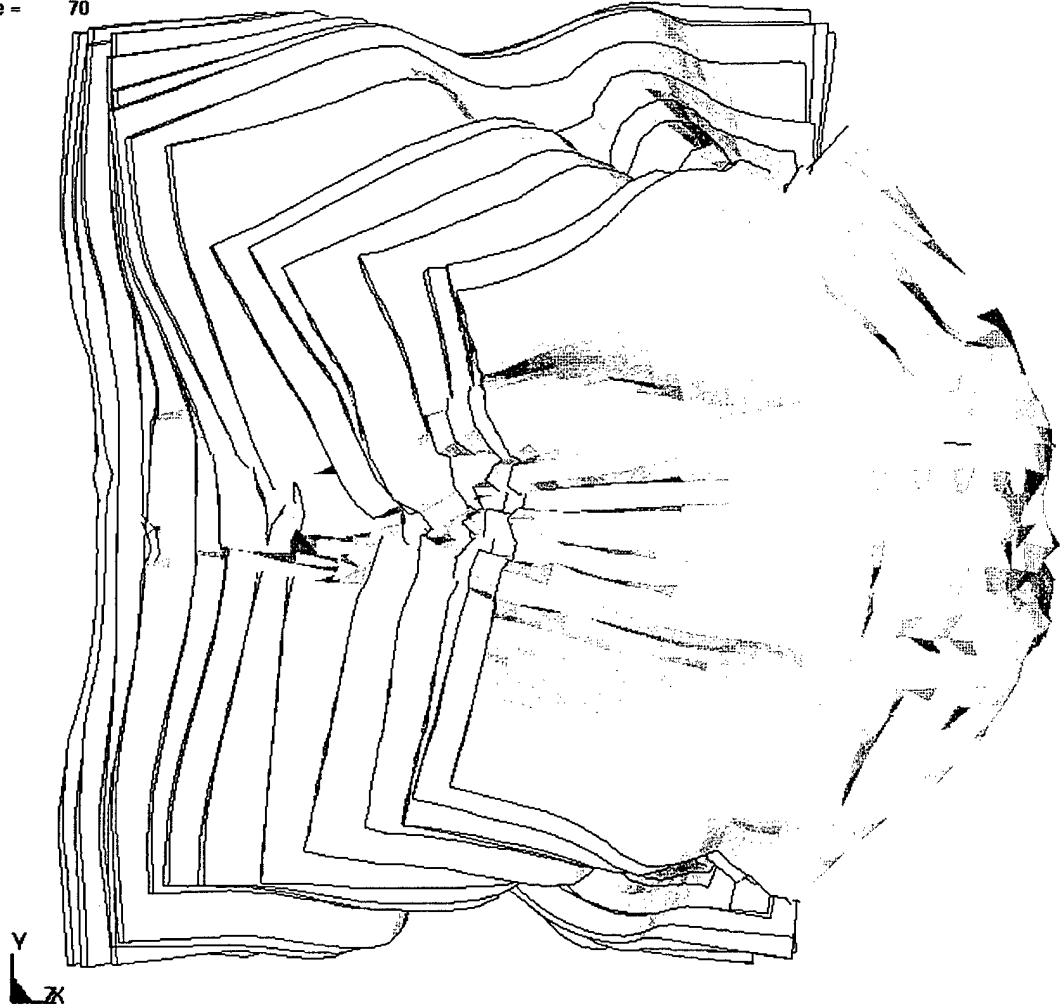


Figure 4. LS-DYNA simulation at 70 μ s into run showing damage up to the sixteenth ply ($V_s = 400$ m/s).

RCC(1.04GM); 0.06 CM/MICROSEC;23PLY KM2
Time = 30

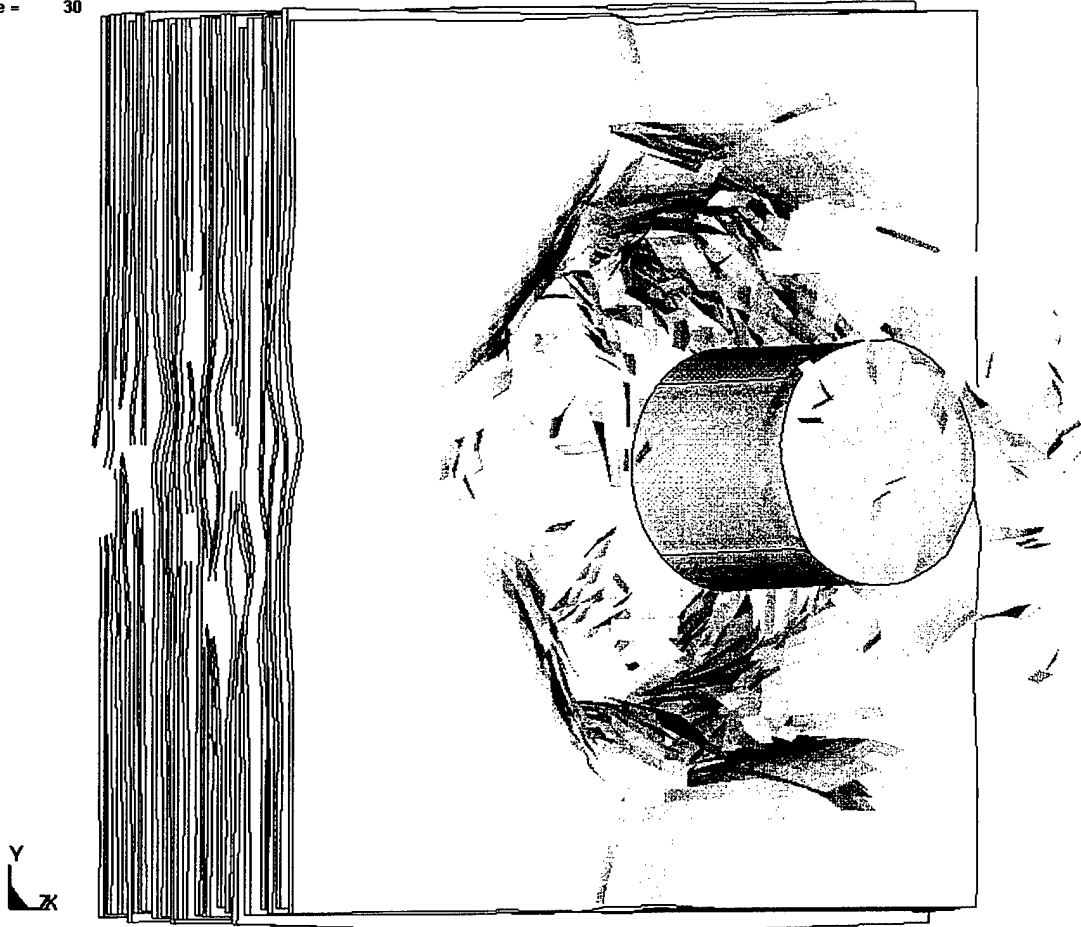


Figure 5. LS-DYNA simulation at 30 μ s into run ($V_s = 600$ m/s).

RCC(1.04GM); 0.08 CM/MICROSEC;23PLY KM2
Time = 30

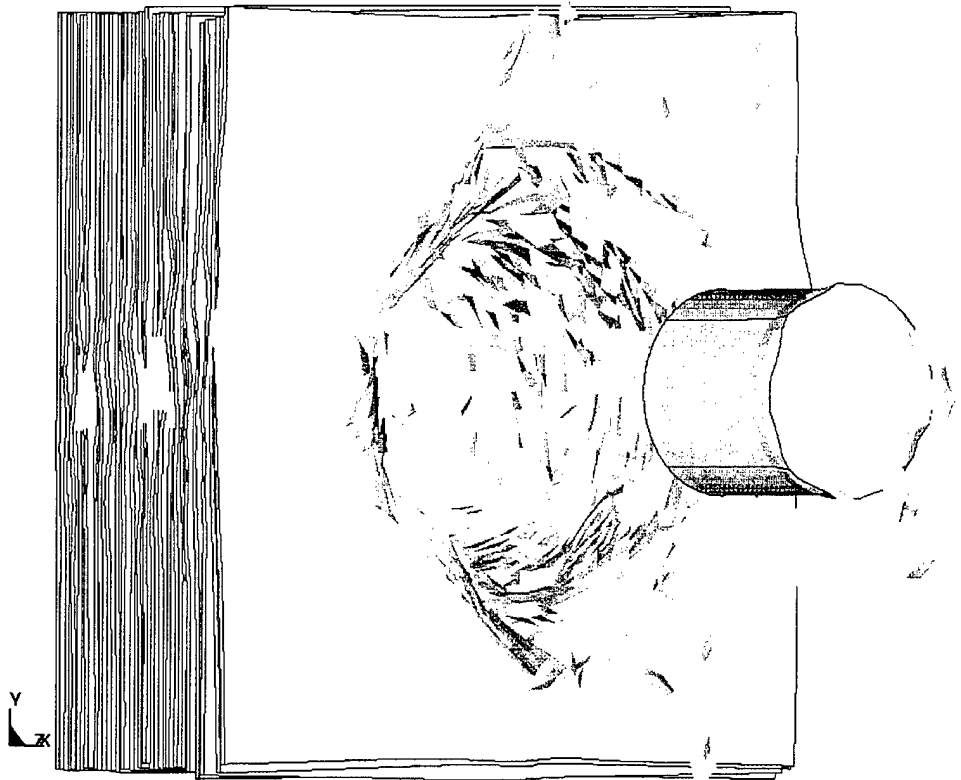


Figure 6. LS-DYNA simulation at 30 μ s into run ($V_s = 800$ m/s).

RCC(1.04GM); 0.10 CM/MICROSEC;23PLY KM2
Time - 25

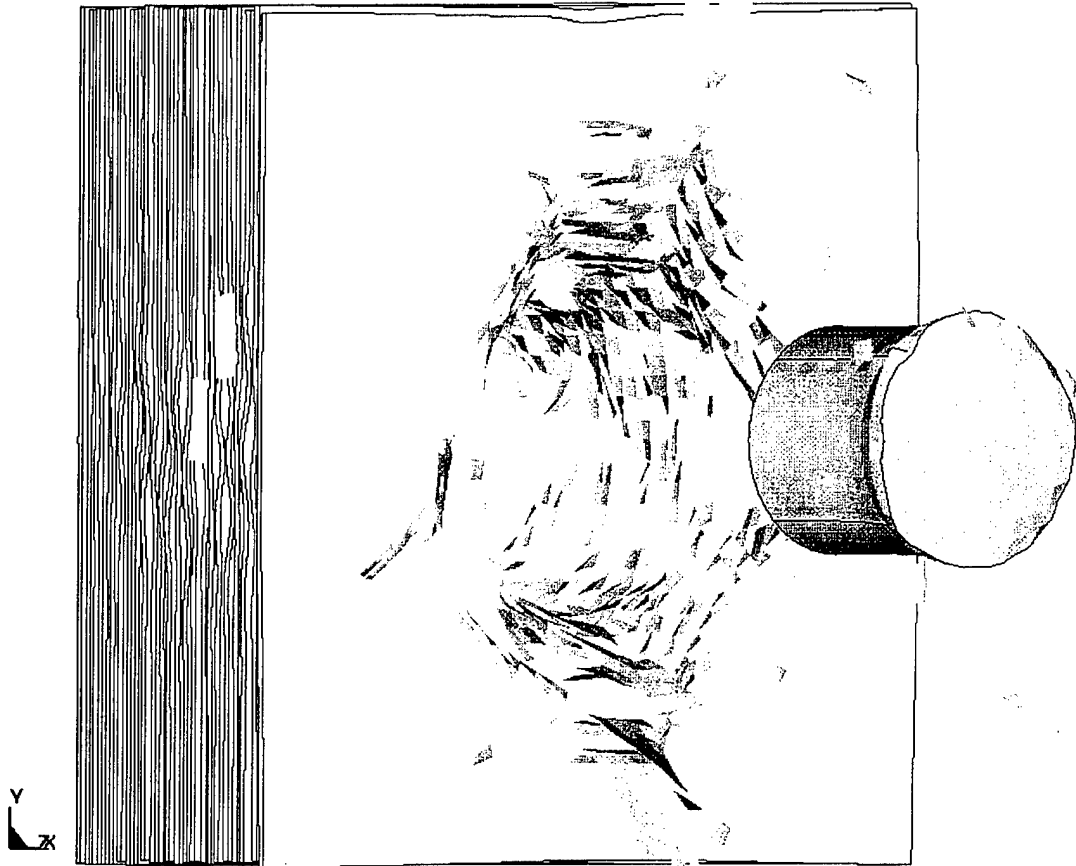


Figure 7. LS-DYNA simulation at 25 μ s into run ($V_s = 1000$ m/s).

RCC(1.04GM); 0.12 CM/MICROSEC;23PLY KM2
Time = 20

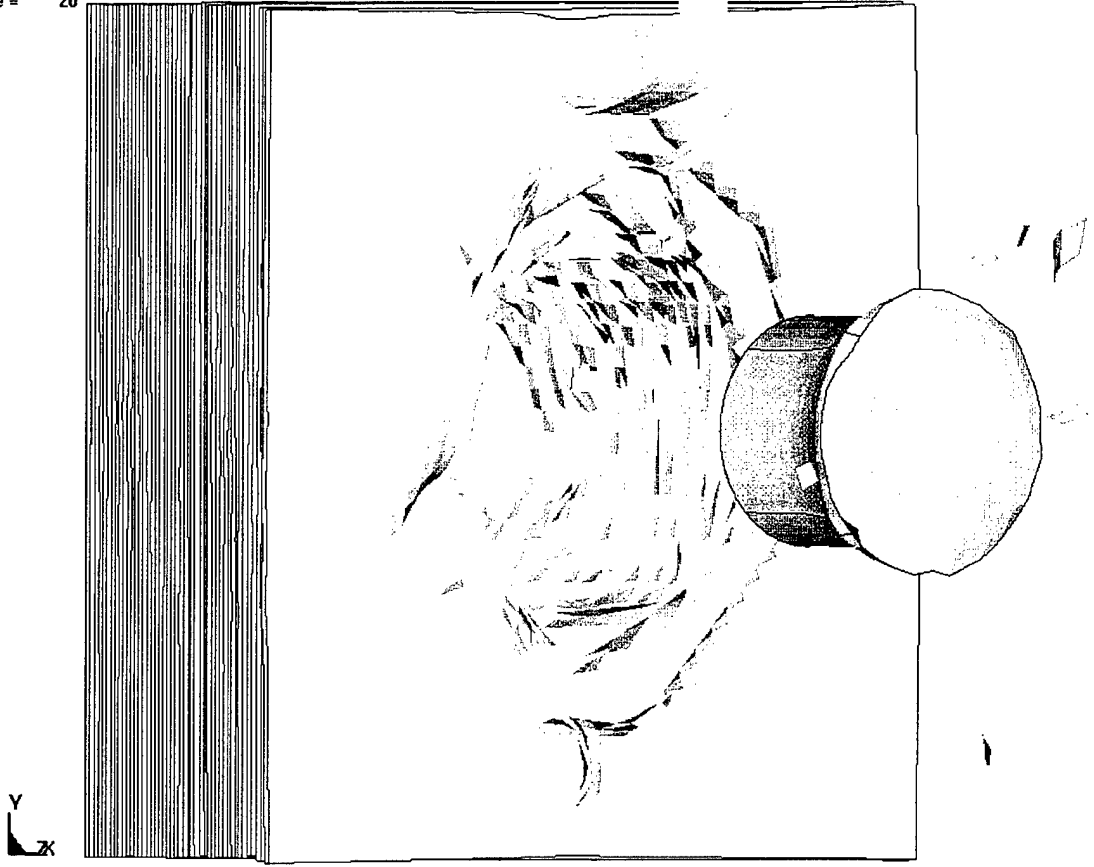


Figure 8. LS-DYNA simulation at 20 μ s into run ($V_s = 1200$ m/s).

RCC(1.04GM); 0.14 CM/MICROSEC;23PLY KM2
Time = 15

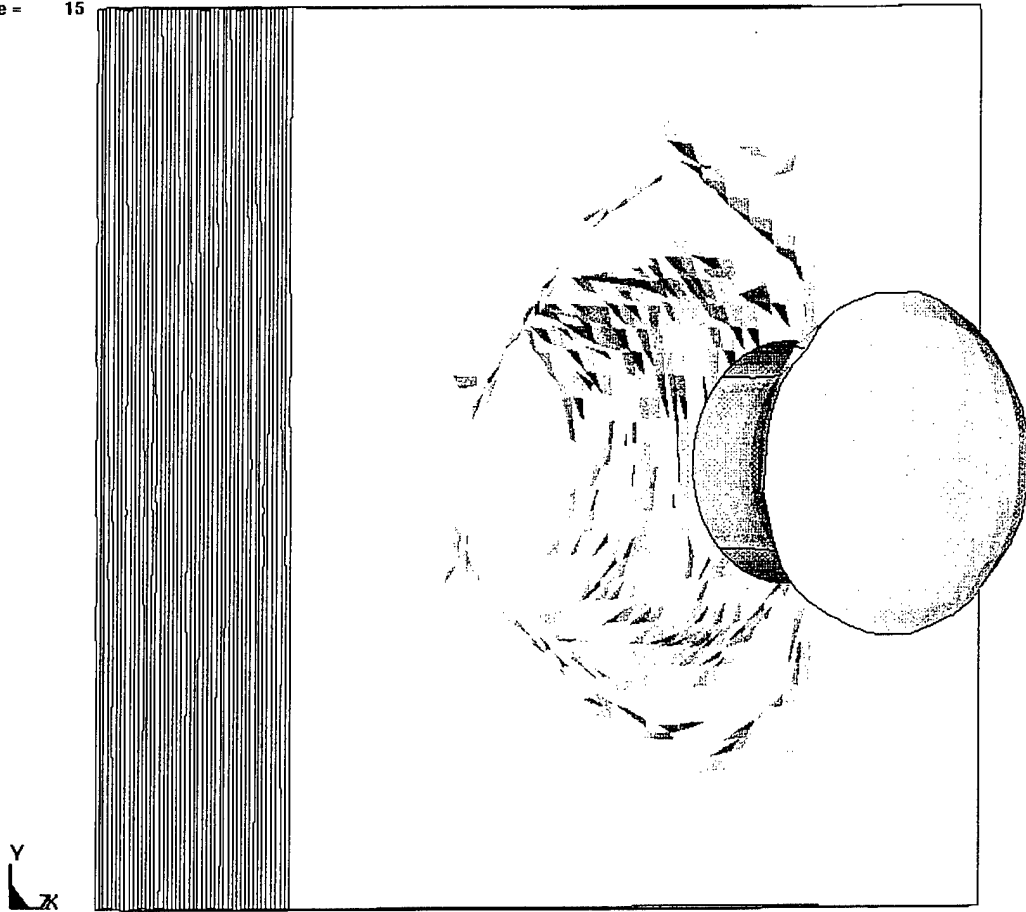


Figure 9. LS-DYNA simulation at 15 μ s into run ($V_s = 1400$ m/s).

variations in the way real fabrics tear in the final penetration process. This effect leads to some penetrators being just caught by the last fabric ply or just making it through that ply with little velocity to spare, given the same V_s . The LS-DYNA computations are flexible, as they allow for the uncertainty of such behavior by letting key input material properties change as required, specifically the Young's modulus and failure strain in Table 2 in this case, accounting for this behavior. Actually, EPIC picked a V_r value that can be thought of as a V_0 value. V_0 is defined as the V_s at which no residual velocity can be obtained. Although EPIC predicted a V_0 in this case, V_0 is not usually obtained experimentally with exacting precision, so its determination to an overly precise number for comparison purposes should not be a computational goal.

3. Summary

The work here forms a baseline for the simulation of fabric penetration by fragment and bullet threats. Future plans include extending the LS-DYNA simulation techniques reported here to a study of 9-mm bullet impact on similar fabric layups. Also, more SHPB testing needs to be sponsored to assist in the process of defining increasingly accurate values for the Young's modulus and failure strain (as functions of strain rate) of KM2 and other ballistic fabrics of interest. This could lead to the development of analytical expressions describing Young's modulus and failure strain as functions of strain rate rather than the first-order discontinuous step model used in the present study. This report demonstrates a technique for reasonably describing the ballistic response of KM2 fabric using the LS-DYNA Lagrangian hydrocode. Using this technique, simulations can be performed to gain additional insight into understanding how the fabric components of armored vests resist ballistic penetration.

INTENTIONALLY LEFT BLANK.

4. References

- Department of the Army. *V₅₀ Ballistic Test for Armor*. MIL-STD-662E, Washington, DC, 27 May 1992.
- Flinn, R. A., and P. K. Trojan. *Engineering Materials and Their Applications*. Boston: Houghton Mifflin, pp. 61 and 72, 1975.
- Johnson, G. R., S. R. Beissel, and P. M. Cunniff. "A Computational Model for Fabrics Subjected to Ballistic Impact." *Proceedings of the 18th International Symposium on Ballistics*, pp. 962-969, San Antonio, TX, November 1999.
- Kolsky, H. *Stress Waves in Solids*. New York: Dover Publications, p. 201, 1963.
- Lyman, T. (editor). *Metals Handbook - 8th Edition, Volume 1: Properties and Selection of Materials*. Metals Park, OH: American Society for Metals, p. 798, 1961.
- Shim, V. P. W., C. T. Lim, and K. J. Foo. "Dynamic Mechanical Properties of Fabric Armour." *International Journal of Impact Engineering*, vol. 25, p. 1-15, 2001.

INTENTIONALLY LEFT BLANK.

**Appendix A. LS-Ingrid Input Deck for RCC and
23-Ply Target**

INTENTIONALLY LEFT BLANK.

```

GRID 1.0 GM RCC AND 23 PLIES KM2
dn3d kw93
c Definition of Parts
start
c ijk notation (Part 1 - Impactor)
1 11;1 11;1 11;
c geometry
0.0545 -0.0545 0.0545 -0.0545 0.000 0.545
a 1 1 1 2 2 2 3 0.2725
C Assign a part number.
mate 1
end
start
c ijk notation (Part 2 - Ply 1)
1 41;1 41;1 2;
c geometry
1.0 -1.0 1.0 -1.0 0.58500 0.60078
c Assign a part number.
mate 2
end
start
c ijk notation (Part 3 - Ply 2)
1 41;1 41;1 2;
1.0 -1.0 1.0 -1.0 0.61469 0.63047
mate 3
end
start
c ijk notation (Part 4 - Ply 3)
1 41;1 41;1 2;
1.0 -1.0 1.0 -1.0 0.64438 0.66016
mate 4
end
start
c ijk notation (Part 5 - Ply 4)
1 41;1 41;1 2;
1.0 -1.0 1.0 -1.0 0.67407 0.68985
mate 5
end
start
c ijk notation (Part 6 - Ply 5)
1 41;1 41;1 2;
1.0 -1.0 1.0 -1.0 0.70376 0.71954
mate 6
end
start
c ijk notation (Part 7 - Ply 6)
1 41;1 41;1 2;
1.0 -1.0 1.0 -1.0 0.73345 0.74923
mate 7
end
start
c ijk notation (Part 8 - Ply 7)
1 41;1 41;1 2;
1.0 -1.0 1.0 -1.0 0.76314 0.77892

```

```

mate 8
end
start
c ijk notation (Part 9 - Ply 8)
1 41;1 41;1 2;
1.0 -1.0 1.0 -1.0 0.79283 0.80861
mate 9
end
start
c ijk notation (Part 10 - Ply 9)
1 41;1 41;1 2;
1.0 -1.0 1.0 -1.0 0.82252 0.83830
mate 10
end
start
c ijk notation (Part 11- Ply 10)
1 41;1 41;1 2;
1.0 -1.0 1.0 -1.0 0.85221 0.86799
mate 11
end
start
c ijk notation (Part 12 - Ply 11)
1 41;1 41;1 2;
1.0 -1.0 1.0 -1.0 0.88190 0.89768
mate 12
end
start
c ijk notation (Part 13 - Ply 12)
1 41;1 41;1 2;
1.0 -1.0 1.0 -1.0 0.91159 0.92737
mate 13
end
start
c ijk notation (Part 14 - Ply 13)
1 41;1 41;1 2;
1.0 -1.0 1.0 -1.0 0.94128 0.95706
mate 14
end
start
c ijk notation (Part 15 - Ply 14)
1 41;1 41;1 2;
1.0 -1.0 1.0 -1.0 0.97097 0.98675
mate 15
end
start
c ijk notation (Part 16 - Ply 15)
1 41;1 41;1 2;
1.0 -1.0 1.0 -1.0 1.00066 1.01644
mate 16
end
start
c ijk notation (Part 17 - Ply 16)
1 41;1 41;1 2;
1.0 -1.0 1.0 -1.0 1.03035 1.04613

```

```
mate 17
end
start
c ijk notation (Part 18 - Ply 17)
1 41;1 41;1 2;
1.0 -1.0 1.0 -1.0 1.06004 1.07582
mate 18
end
start
c ijk notation (Part 19 - Ply 18)
1 41;1 41;1 2;
1.0 -1.0 1.0 -1.0 1.08973 1.10551
mate 19
end
start
c ijk notation (Part 20 - Ply 19)
1 41;1 41;1 2;
1.0 -1.0 1.0 -1.0 1.11942 1.13520
mate 20
end
start
c ijk notation (Part 21 - Ply 20)
1 41;1 41;1 2;
1.0 -1.0 1.0 -1.0 1.14911 1.16489
mate 21
end
start
c ijk notation (Part 22 - Ply 21)
1 41;1 41;1 2;
1.0 -1.0 1.0 -1.0 1.17880 1.19458
mate 22
end
start
c ijk notation (Part 23 - Ply 22)
1 41;1 41;1 2;
1.0 -1.0 1.0 -1.0 1.20849 1.22427
mate 23
end
start
c ijk notation (Part 24 - Ply 23)
1 41;1 41;1 2;
1.0 -1.0 1.0 -1.0 1.23818 1.25396
mate 24
end
end
```

INTENTIONALLY LEFT BLANK.

**Appendix B. Abbreviated LS-DYNA Input Deck for RCC
Impacting 23-Ply Target ($V_s = 200$ m/s)**

INTENTIONALLY LEFT BLANK.


```

      1      2      3      3
$   fric
    0.0
$   sfs
    1.0
$   isym   erosop
      1     1
$
*CONTACT_ERODING_SURFACE_TO_SURFACE
$   ssid   msid   sstyp   mstyp
      1     3     3     3
$   fric
    0.0
$   sfs
    1.0
$   isym   erosop
      1     1
$
*CONTACT_ERODING_SURFACE_TO_SURFACE
$   ssid   msid   sstyp   mstyp
      1     4     3     3
$   fric
    0.0
$   sfs
    1.0
$   isym   erosop
      1     1
$
*CONTACT_ERODING_SURFACE_TO_SURFACE
$   ssid   msid   sstyp   mstyp
      1     5     3     3
$   fric
    0.0
$   sfs
    1.0
$   isym   erosop
      1     1
$
*CONTACT_ERODING_SURFACE_TO_SURFACE
$   ssid   msid   sstyp   mstyp
      1     6     3     3
$   fric
    0.0
$   sfs
    1.0
$   isym   erosop
      1     1
$
*CONTACT_ERODING_SURFACE_TO_SURFACE
$   ssid   msid   sstyp   mstyp
      1     7     3     3
$   fric
    0.0
$   sfs
    1.0
$   isym   erosop
      1     1
$
*CONTACT_ERODING_SURFACE_TO_SURFACE
$   ssid   msid   sstyp   mstyp
      1     8     3     3
$   fric
    0.0
$   sfs
    1.0
$   isym   erosop
      1     1
$

```

```

*CONTACT_ERODING_SURFACE_TO_SURFACE
$  ssid      msid      sstyp      mstyp
  1          9         3          3
$  fric
  0.0
$  sfs
  1.0
$  isym      erosop
  1          1
$
*CONTACT_ERODING_SURFACE_TO_SURFACE
$  ssid      msid      sstyp      mstyp
  1         10         3          3
$  fric
  0.0
$  sfs
  1.0
$  isym      erosop
  1          1
$
*CONTACT_ERODING_SURFACE_TO_SURFACE
$  ssid      msid      sstyp      mstyp
  1         11         3          3
$  fric
  0.0
$  sfs
  1.0
$  isym      erosop
  1          1
$
*CONTACT_ERODING_SURFACE_TO_SURFACE
$  ssid      msid      sstyp      mstyp
  1         12         3          3
$  fric
  0.0
$  sfs
  1.0
$  isym      erosop
  1          1
$
*CONTACT_ERODING_SURFACE_TO_SURFACE
$  ssid      msid      sstyp      mstyp
  1         13         3          3
$  fric
  0.0
$  sfs
  1.0
$  isym      erosop
  1          1
$
*CONTACT_ERODING_SURFACE_TO_SURFACE
$  ssid      msid      sstyp      mstyp
  1         14         3          3
$  fric
  0.0
$  sfs
  1.0
$  isym      erosop
  1          1
$
*CONTACT_ERODING_SURFACE_TO_SURFACE
$  ssid      msid      sstyp      mstyp
  1         15         3          3
$  fric
  0.0
$  sfs
  1.0
$  isym      erosop

```

```

      1      1
$
*CONTACT_ERODING_SURFACE_TO_SURFACE
$  ssid      msid      sstyp      mstyp
   1         16         3         3
$  fric
   0.0
$  sfs
   1.0
$  isym      erosop
   1         1
$
*CONTACT_ERODING_SURFACE_TO_SURFACE
$  ssid      msid      sstyp      mstyp
   1         17         3         3
$  fric
   0.0
$  sfs
   1.0
$  isym      erosop
   1         1
$
*CONTACT_ERODING_SURFACE_TO_SURFACE
$  ssid      msid      sstyp      mstyp
   1         18         3         3
$  fric
   0.0
$  sfs
   1.0
$  isym      erosop
   1         1
$
*CONTACT_ERODING_SURFACE_TO_SURFACE
$  ssid      msid      sstyp      mstyp
   1         19         3         3
$  fric
   0.0
$  sfs
   1.0
$  isym      erosop
   1         1
$
*CONTACT_ERODING_SURFACE_TO_SURFACE
$  ssid      msid      sstyp      mstyp
   1         20         3         3
$  fric
   0.0
$  sfs
   1.0
$  isym      erosop
   1         1
$
*CONTACT_ERODING_SURFACE_TO_SURFACE
$  ssid      msid      sstyp      mstyp
   1         21         3         3
$  fric
   0.0
$  sfs
   1.0
$  isym      erosop
   1         1
$
*CONTACT_ERODING_SURFACE_TO_SURFACE
$  ssid      msid      sstyp      mstyp
   1         22         3         3
$  fric
   0.0
$  sfs

```

```

    1.0
$   isym   erosop
    1       1
$
*CONTACT_ERODING_SURFACE_TO_SURFACE
$   ssid   msid   sstyp   mstyp
    1       23      3       3
$   fric
    0.0
$   sfs
    1.0
$   isym   erosop
    1       1
$
*CONTACT_ERODING_SURFACE_TO_SURFACE
$   ssid   msid   sstyp   mstyp
    1       24      3       3
$   fric
    0.0
$   sfs
    1.0
$   isym   erosop
    1       1
$
$initiate master-slave routine for each ply $$$$$$$$$$$$$$$$$$$$$$$$$$$$$$$$$
$
*CONTACT_ERODING_SURFACE_TO_SURFACE
$   ssid   msid   sstyp   mstyp
    2       3       3       3
$   fric
    0.0
$   sfs
    1.0
$   isym   erosop
    1       1
$
*CONTACT_ERODING_SURFACE_TO_SURFACE
$   ssid   msid   sstyp   mstyp
    2       4       3       3
$   fric
    0.0
$   sfs
    1.0
$   isym   erosop
    1       1
$
*CONTACT_ERODING_SURFACE_TO_SURFACE
$   ssid   msid   sstyp   mstyp
    3       4       3       3
$   fric
    0.0
$   sfs
    1.0
$   isym   erosop
    1       1
$
*CONTACT_ERODING_SURFACE_TO_SURFACE
$   ssid   msid   sstyp   mstyp
    3       5       3       3
$   fric
    0.0
$   sfs
    1.0
$   isym   erosop
    1       1
$
*CONTACT_ERODING_SURFACE_TO_SURFACE
$   ssid   msid   sstyp   mstyp

```

```

      4      5      3      3
$   fric
   0.0
$   sfs
   1.0
$   isym   erosop
      1     1
$
*CONTACT_ERODING_SURFACE_TO_SURFACE
$   ssid   msid   sstyp   mstyp
      4     6     3     3
$   fric
   0.0
$   sfs
   1.0
$   isym   erosop
      1     1
$
*CONTACT_ERODING_SURFACE_TO_SURFACE
$   ssid   msid   sstyp   mstyp
      5     6     3     3
$   fric
   0.0
$   sfs
   1.0
$   isym   erosop
      1     1
$
*CONTACT_ERODING_SURFACE_TO_SURFACE
$   ssid   msid   sstyp   mstyp
      5     7     3     3
$   fric
   0.0
$   sfs
   1.0
$   isym   erosop
      1     1
$
*CONTACT_ERODING_SURFACE_TO_SURFACE
$   ssid   msid   sstyp   mstyp
      6     7     3     3
$   fric
   0.0
$   sfs
   1.0
$   isym   erosop
      1     1
$
*CONTACT_ERODING_SURFACE_TO_SURFACE
$   ssid   msid   sstyp   mstyp
      6     8     3     3
$   fric
   0.0
$   sfs
   1.0
$   isym   erosop
      1     1
$
*CONTACT_ERODING_SURFACE_TO_SURFACE
$   ssid   msid   sstyp   mstyp
      7     8     3     3
$   fric
   0.0
$   sfs
   1.0
$   isym   erosop
      1     1
$

```

```

*CONTACT_ERODING_SURFACE_TO_SURFACE
$  ssid      msid      sstyp      mstyp
   7         9         3         3
$  fric
   0.0
$  sfs
   1.0
$  isym      erosop
   1         1
$
*CONTACT_ERODING_SURFACE_TO_SURFACE
$  ssid      msid      sstyp      mstyp
   8         9         3         3
$  fric
   0.0
$  sfs
   1.0
$  isym      erosop
   1         1
$
*CONTACT_ERODING_SURFACE_TO_SURFACE
$  ssid      msid      sstyp      mstyp
   8         10        3         3
$  fric
   0.0
$  sfs
   1.0
$  isym      erosop
   1         1
$
*CONTACT_ERODING_SURFACE_TO_SURFACE
$  ssid      msid      sstyp      mstyp
   9         10        3         3
$  fric
   0.0
$  sfs
   1.0
$  isym      erosop
   1         1
$
*CONTACT_ERODING_SURFACE_TO_SURFACE
$  ssid      msid      sstyp      mstyp
   9         11        3         3
$  fric
   0.0
$  sfs
   1.0
$  isym      erosop
   1         1
$
*CONTACT_ERODING_SURFACE_TO_SURFACE
$  ssid      msid      sstyp      mstyp
  10         11        3         3
$  fric
   0.0
$  sfs
   1.0
$  isym      erosop
   1         1
$
*CONTACT_ERODING_SURFACE_TO_SURFACE
$  ssid      msid      sstyp      mstyp
  10         12        3         3
$  fric
   0.0
$  sfs
   1.0
$  isym      erosop

```

```

      1      1
$
*CONTACT_ERODING_SURFACE_TO_SURFACE
$  ssid      msid      sstyp      mstyp
   11        12        3          3
$  fric
   0.0
$  sfs
   1.0
$  isym      erosop
   1          1
$
*CONTACT_ERODING_SURFACE_TO_SURFACE
$  ssid      msid      sstyp      mstyp
   11        13        3          3
$  fric
   0.0
$  sfs
   1.0
$  isym      erosop
   1          1
$
*CONTACT_ERODING_SURFACE_TO_SURFACE
$  ssid      msid      sstyp      mstyp
   12        13        3          3
$  fric
   0.0
$  sfs
   1.0
$  isym      erosop
   1          1
$
*CONTACT_ERODING_SURFACE_TO_SURFACE
$  ssid      msid      sstyp      mstyp
   12        14        3          3
$  fric
   0.0
$  sfs
   1.0
$  isym      erosop
   1          1
$
*CONTACT_ERODING_SURFACE_TO_SURFACE
$  ssid      msid      sstyp      mstyp
   13        14        3          3
$  fric
   0.0
$  sfs
   1.0
$  isym      erosop
   1          1
$
*CONTACT_ERODING_SURFACE_TO_SURFACE
$  ssid      msid      sstyp      mstyp
   13        15        3          3
$  fric
   0.0
$  sfs
   1.0
$  isym      erosop
   1          1
$
*CONTACT_ERODING_SURFACE_TO_SURFACE
$  ssid      msid      sstyp      mstyp
   14        15        3          3
$  fric
   0.0
$  sfs
   1.0

```

```

$ isym erosop
  1      1
$
*CONTACT_ERODING_SURFACE_TO_SURFACE
$ ssid      msid      sstyp      mstyp
  14        16        3          3
$ fric
  0.0
$ sfs
  1.0
$ isym erosop
  1      1
$
*CONTACT_ERODING_SURFACE_TO_SURFACE
$ ssid      msid      sstyp      mstyp
  15        16        3          3
$ fric
  0.0
$ sfs
  1.0
$ isym erosop
  1      1
$
*CONTACT_ERODING_SURFACE_TO_SURFACE
$ ssid      msid      sstyp      mstyp
  15        17        3          3
$ fric
  0.0
$ sfs
  1.0
$ isym erosop
  1      1
$
*CONTACT_ERODING_SURFACE_TO_SURFACE
$ ssid      msid      sstyp      mstyp
  16        17        3          3
$ fric
  0.0
$ sfs
  1.0
$ isym erosop
  1      1
$
*CONTACT_ERODING_SURFACE_TO_SURFACE
$ ssid      msid      sstyp      mstyp
  16        18        3          3
$ fric
  0.0
$ sfs
  1.0
$ isym erosop
  1      1
$
*CONTACT_ERODING_SURFACE_TO_SURFACE
$ ssid      msid      sstyp      mstyp
  17        18        3          3
$ fric
  0.0
$ sfs
  1.0
$ isym erosop
  1      1
$
*CONTACT_ERODING_SURFACE_TO_SURFACE
$ ssid      msid      sstyp      mstyp
  17        19        3          3
$ fric
  0.0
$ sfs

```

```

    1.0
$   isym   erosop
    1       1
$
*CONTACT_ERODING_SURFACE_TO_SURFACE
$   ssid   msid   sstyp   mstyp
    18     19     3       3
$   fric
    0.0
$   sfs
    1.0
$   isym   erosop
    1       1
$
*CONTACT_ERODING_SURFACE_TO_SURFACE
$   ssid   msid   sstyp   mstyp
    18     20     3       3
$   fric
    0.0
$   sfs
    1.0
$   isym   erosop
    1       1
$
*CONTACT_ERODING_SURFACE_TO_SURFACE
$   ssid   msid   sstyp   mstyp
    19     20     3       3
$   fric
    0.0
$   sfs
    1.0
$   isym   erosop
    1       1
$
*CONTACT_ERODING_SURFACE_TO_SURFACE
$   ssid   msid   sstyp   mstyp
    19     21     3       3
$   fric
    0.0
$   sfs
    1.0
$   isym   erosop
    1       1
$
*CONTACT_ERODING_SURFACE_TO_SURFACE
$   ssid   msid   sstyp   mstyp
    20     21     3       3
$   fric
    0.0
$   sfs
    1.0
$   isym   erosop
    1       1
$
*CONTACT_ERODING_SURFACE_TO_SURFACE
$   ssid   msid   sstyp   mstyp
    20     22     3       3
$   fric
    0.0
$   sfs
    1.0
$   isym   erosop
    1       1
$
*CONTACT_ERODING_SURFACE_TO_SURFACE
$   ssid   msid   sstyp   mstyp
    21     22     3       3
$   fric

```

```

0.0
$   sfs
   1.0
$   isym   erosop
       1       1
$
*CONTACT_ERODING_SURFACE_TO_SURFACE
$   ssid   msid   sstyp   mstyp
       21       23       3       3
$   fric
       0.0
$   sfs
       1.0
$   isym   erosop
       1       1
$
*CONTACT_ERODING_SURFACE_TO_SURFACE
$   ssid   msid   sstyp   mstyp
       22       23       3       3
$   fric
       0.0
$   sfs
       1.0
$   isym   erosop
       1       1
$
*CONTACT_ERODING_SURFACE_TO_SURFACE
$   ssid   msid   sstyp   mstyp
       22       24       3       3
$   fric
       0.0
$   sfs
       1.0
$   isym   erosop
       1       1
$
*CONTACT_ERODING_SURFACE_TO_SURFACE
$   ssid   msid   sstyp   mstyp
       23       24       3       3
$   fric
       0.0
$   sfs
       1.0
$   isym   erosop
       1       1
$
*INITIAL_VELOCITY_GENERATION
$   sid   styp   omega   vx   vy   vz
       1       1           0.02
$   xc   yc   zc
$
*SET_PART
$   setid
       1
$   pid1
       1
$
*PART
$   pid   sid   mid
16 gr RCC
       1       1       1
1st ply of KM2
       2       1       2
2nd ply of KM2
       3       1       2
3rd ply of KM2
       4       1       2

```


2	1.601715088E-01	2.204571813E-01	0.000000000E+00	0	0
3	1.237124354E-01	2.427993417E-01	0.000000000E+00	0	0
4	8.420714736E-02	2.591629624E-01	0.000000000E+00	0	0
5	4.262839630E-02	2.691451609E-01	0.000000000E+00	0	0
6	-1.056444709E-08	2.725000679E-01	0.000000000E+00	0	0
7	-4.262841865E-02	2.691451609E-01	0.000000000E+00	0	0
8	-8.420717716E-02	2.591629922E-01	0.000000000E+00	0	0
9	-1.237124726E-01	2.427993566E-01	0.000000000E+00	0	0
10	-1.601715535E-01	2.204572111E-01	0.000000000E+00	0	0
11	-1.926866323E-01	1.926866323E-01	0.000000000E+00	0	0
12	2.204571813E-01	1.601715088E-01	0.000000000E+00	0	0

NOTE: THE MISSING NODES IN THIS ABBREVIATED DECK ARE HERE IN THE ACTUAL RUN

78646	-4.499999881E-01	-1.000000000E+00	1.253960252E+00	0	0
78647	-5.000000000E-01	-1.000000000E+00	1.253960252E+00	0	0
78648	-5.500000119E-01	-1.000000000E+00	1.253960252E+00	0	0
78649	-6.000000238E-01	-1.000000000E+00	1.253960252E+00	0	0
78650	-6.499999762E-01	-1.000000000E+00	1.253960252E+00	0	0
78651	-6.999999881E-01	-1.000000000E+00	1.253960252E+00	0	0
78652	-7.500000000E-01	-1.000000000E+00	1.253960252E+00	0	0
78653	-8.000000119E-01	-1.000000000E+00	1.253960252E+00	0	0
78654	-8.500000238E-01	-1.000000000E+00	1.253960252E+00	0	0
78655	-8.999999762E-01	-1.000000000E+00	1.253960252E+00	0	0
78656	-9.499999881E-01	-1.000000000E+00	1.253960252E+00	0	0
78657	-1.000000000E+00	-1.000000000E+00	1.253960252E+00	0	0

*ELEMENT_SOLID

1	1	1	2	13	12	122	123	134	133
2	1	2	3	14	13	123	124	135	134
3	1	3	4	15	14	124	125	136	135
4	1	4	5	16	15	125	126	137	136
5	1	5	6	17	16	126	127	138	137
6	1	6	7	18	17	127	128	139	138
7	1	7	8	19	18	128	129	140	139
8	1	8	9	20	19	129	130	141	140
9	1	9	10	21	20	130	131	142	141
10	1	10	11	22	21	131	132	143	142
11	1	12	13	24	23	133	134	145	144
12	1	13	14	25	24	134	135	146	145

NOTE: THE MISSING SOLID ELEMENTS IN THIS ABBREVIATED DECK ARE HERE IN THE ACTUAL RUN

37789	24	76923	76924	76965	76964	78604	78605	78646	78645
37790	24	76924	76925	76966	76965	78605	78606	78647	78646
37791	24	76925	76926	76967	76966	78606	78607	78648	78647
37792	24	76926	76927	76968	76967	78607	78608	78649	78648
37793	24	76927	76928	76969	76968	78608	78609	78650	78649
37794	24	76928	76929	76970	76969	78609	78610	78651	78650
37795	24	76929	76930	76971	76970	78610	78611	78652	78651
37796	24	76930	76931	76972	76971	78611	78612	78653	78652
37797	24	76931	76932	76973	76972	78612	78613	78654	78653
37798	24	76932	76933	76974	76973	78613	78614	78655	78654
37799	24	76933	76934	76975	76974	78614	78615	78656	78655
37800	24	76934	76935	76976	76975	78615	78616	78657	78656

*END

INTENTIONALLY LEFT BLANK.

<u>NO. OF COPIES</u>	<u>ORGANIZATION</u>
2	DEFENSE TECHNICAL INFORMATION CENTER DTIC OCA 8725 JOHN J KINGMAN RD STE 0944 FT BELVOIR VA 22060-6218
1	HQDA DAMO FDT 400 ARMY PENTAGON WASHINGTON DC 20310-0460
1	OSD OUSD(A&T)/ODDR&E(R) DR R J TREW 3800 DEFENSE PENTAGON WASHINGTON DC 20301-3800
1	COMMANDING GENERAL US ARMY MATERIEL CMD AMCRDA TF 5001 EISENHOWER AVE ALEXANDRIA VA 22333-0001
1	INST FOR ADVNCD TCHNLGY THE UNIV OF TEXAS AT AUSTIN 3925 W BRAKER LN STE 400 AUSTIN TX 78759-5316
1	US MILITARY ACADEMY MATH SCI CTR EXCELLENCE MADN MATH THAYER HALL WEST POINT NY 10996-1786
1	DIRECTOR US ARMY RESEARCH LAB AMSRL D DR D SMITH 2800 POWDER MILL RD ADELPHI MD 20783-1197
1	DIRECTOR US ARMY RESEARCH LAB AMSRL CI AI R 2800 POWDER MILL RD ADELPHI MD 20783-1197

<u>NO. OF COPIES</u>	<u>ORGANIZATION</u>
3	DIRECTOR US ARMY RESEARCH LAB AMSRL CI LL 2800 POWDER MILL RD ADELPHI MD 20783-1197
3	DIRECTOR US ARMY RESEARCH LAB AMSRL CI IS T 2800 POWDER MILL RD ADELPHI MD 20783-1197
	<u>ABERDEEN PROVING GROUND</u>
2	DIR USARL AMSRL CI LP (BLDG 305)

<u>NO. OF COPIES</u>	<u>ORGANIZATION</u>
4	COMMANDER US ARMY ARDEC T HAAR R MAHTOOK R MAZESKI R MCHUGH PICATINNY ARSENAL NJ 07806-5000
3	COMMANDER US ARMY NGIC T SHAVER J CRIDER J LILLY 220 SEVENTH ST NE CHARLOTTESVILLE VA 22902-5396
2	COMMANDER US ARMY RESEARCH OFFICE K IYER J BAILEY P O BOX 12211 RSRCH TRIANGLE PARK NC 27709-2211
2	COMMANDER US ARMY TARDEC R GOODMAN G BAKER WARREN MI 48397-5000
1	COMMANDER PM SOLDIER B KIRKWOOD FORT BELVOIR VA 22060
1	COMMANDER NAVAL POSTGRADUATE SCHOOL J STERNBERG MONTEREY CA 93943
5	COMMANDER US ARMY SOLDIER SYSTEMS CTR J WARD P CUNNIFF S WACLAWIK J MACKIEWICZ S BENNETT NATICK MA 01706-5010

<u>NO. OF COPIES</u>	<u>ORGANIZATION</u>
	<u>ABERDEEN PROVING GROUND</u>
23	DIR USARL AMSRL CI HC D GROVE AMSRL SL BE J LIU AMSRL SL BG J PLOSKONKA AMSRL WM MB T BOGETTI B CHEESEMAN C HOPPEL AMSRL WM TA W GILLICH T HAVEL AMSRL WM TB P BAKER W LAWRENCE AMSRL WM TC G SILSBY R SUMMERS W WALTERS AMSRL WM TD T HADUCH D PRITCHARD (6 CPS) M RAFTENBURG E RAPACKI S SCHOENFELD

REPORT DOCUMENTATION PAGE			Form Approved OMB No. 0704-0188	
Public reporting burden for this collection of information is estimated to average 1 hour per response, including the time for reviewing instructions, searching existing data sources, gathering and maintaining the data needed, and completing and reviewing the collection of information. Send comments regarding this burden estimate or any other aspect of this collection of information, including suggestions for reducing this burden, to Washington Headquarters Services, Directorate for Information Operations and Reports, 1215 Jefferson Davis Highway, Suite 1204, Arlington, VA 22202-4302, and to the Office of Management and Budget, Paperwork Reduction Project(0704-0188), Washington, DC 20503.				
1. AGENCY USE ONLY (Leave blank)	2. REPORT DATE February 2002	3. REPORT TYPE AND DATES COVERED Final, October 2000 – September 2001		
4. TITLE AND SUBTITLE A Study of a Steel Right Circular Cylinder (RCC) Striking 23 Plies of KM2 Fabric Using the LS-DYNA Lagrangian Hydrocode		5. FUNDING NUMBERS 622105AH84		
6. AUTHOR(S) Dennis S. Pritchard				
7. PERFORMING ORGANIZATION NAME(S) AND ADDRESS(ES) U.S. Army Research Laboratory ATTN: AMSRL-WM-TD Aberdeen Proving Ground, MD 21005-5066		8. PERFORMING ORGANIZATION REPORT NUMBER ARL-TR-2673		
9. SPONSORING/MONITORING AGENCY NAMES(S) AND ADDRESS(ES)		10. SPONSORING/MONITORING AGENCY REPORT NUMBER		
11. SUPPLEMENTARY NOTES				
12a. DISTRIBUTION/AVAILABILITY STATEMENT Approved for public release; distribution is unlimited.		12b. DISTRIBUTION CODE		
13. ABSTRACT (Maximum 200 words) A study was conducted to examine the terminal effects of a 1.0-g steel RCC impacting 23 plies of KM2 fabric using the LS-DYNA Lagrangian hydrocode. The simulated impact velocities were 200, 400, 600, 800, 1000, 1200, and 1400 m/s. The fabric was a plain weave of 850 denier yarn. The LS-DYNA-simulated V_s versus V_r data points generated at the U.S. Army Research Laboratory (ARL) were compared to both experimental data and EPIC-generated data. Also, the LS-POST software package was used to view the simulated physical descriptions of the penetrator and target at various stages of the penetration process.				
14. SUBJECT TERMS steel, right circular cylinder, RCC, KM2, fabric, LS-DYNA, Lagrangian hydrocode, striking velocity, residual velocity, simulation, impact, fragment, penetration		15. NUMBER OF PAGES 43		16. PRICE CODE
17. SECURITY CLASSIFICATION OF REPORT UNCLASSIFIED	18. SECURITY CLASSIFICATION OF THIS PAGE UNCLASSIFIED	19. SECURITY CLASSIFICATION OF ABSTRACT UNCLASSIFIED	20. LIMITATION OF ABSTRACT UL	

INTENTIONALLY LEFT BLANK.